HEAVY METAL-CONTAMINATED SOIL REMEDIATION THROUGH EDEM BASED ON ROTARY TILLAGE

Fu, C. G.[*,**,#]; He, W. W.[**]; Li, Y. H.[***] & Lv, W. Q.[****]

[*] School of Mechanical Engineering, Guizhou University of Engineering Science, Bijie, 551700, China
[**] School of Electrical and Mechanical Engineering, Henan Institute of Science and Technology, Xinxiang, 453000, China
[***] School of Engineering, South China Agricultural University, Guangzhou, 510640, China
[****] College of Engineering China, Agricultural University, Beijing, 100083, China
E-Mail: scu_fcg@163.com ([#] Corresponding author)

Abstract

To address the technical challenge of the uneven distribution of passivator particles (more in the upper layer and less in the lower layer) during the chemical remediation of heavy metal-contaminated soil, this study proposed a method based on rotary tillage for mixing passivator particles with soil. Initially, the key structure of the rotary tiller was optimized, and the tillage process was numerically simulated using the Enhanced Discrete Element Method (EDEM). Taking the mixing uniformity of passivator particles and soil particles as the core evaluation metric, and under a fixed tillage depth of 25 cm, the travel speed of the rotary tiller and the blade roller speed were selected as key variables. Results demonstrate that when the travel speed of the rotary tiller is maintained at 2 km/h and the blade roller speed is set to 250 r/min, the mixing uniformity of passivator and soil particles reaches 82 % after secondary tillage, representing 61 % improvement compared to primary tillage. The proposed method provides a crucial evidence for the optimization of soil remediation processes, which has significant academic and practical implications.
(Received in October 2024, accepted in January 2025. This paper was with the authors 1 month for 2 revisions.)

1. INTRODUCTION

The health of the soil, which serves as an important foundation for agricultural production, is a prerequisite for sustainable agricultural development and human health. However, in recent years, heavy metal pollution in farmland soils has become increasingly severe due to human activities. These activities include intensive agricultural practices, such as the excessive use of pesticides and chemical fertilizers, and industrial activities, such as the large-scale emission of heavy metal–containing waste water, waste gas, and solid waste from enterprises [1, 2]. The remediation of heavy metal-contaminated soil has become a major global environmental challenge. More than 5 million hectares of land worldwide have been contaminated by heavy metals. For example, in China, India, and Egypt, the concentrations of cadmium (Cd), arsenic (As), and lead (Pb) in a significant portion of the soil exceed the threshold limit value of heavy metals in soil. Millions of hectares of farmland in Europe are contaminated by heavy metals, and in Japan the area of farmland contaminated by heavy metals such as Cd and copper (Cu) is 7.3×10^9 m^2 [3]. In 2014, the Bulletin of National Soil Pollution Survey issued by the Chinese government showed that the total point location overlimit rate of soil pollution in China reached 16.1 %, of which the overlimit rate of cultivated land was 19.4 %, and the pollution was mainly caused by heavy metals such as Cd, As, and mercury (Hg) [4]. Crops can absorb and accumulate heavy metals from soil through their roots thereby posing a potential threat to human health via food chain. Heavy metal pollution in farmland soil thus has seriously endangered food security and human health [5]. Therefore, the remediation of heavy metal-contaminated soil has become one of the primary tasks in soil management.

To minimize the harm of heavy metals, contaminated soil remediation has been extensively investigated by several scholars. The key strategies include reducing the absorption and fixation of heavy metals by crops or remove heavy metals [6, 7]. Currently, the main remediation measures include: (1) the selection and breeding of low-metal varieties, (2) physiological blockades, (3) moisture management, (4) soil amendments, and (5) phytoremediation [8, 9]. Among these measures, soil improvement, as the most common way of soil remediation, involves the mixing and blending of soil and heavy metal passivator agents in the soil remediation unit, and the remediation effectiveness is directly influenced by the mixing uniformity [10]. The practical remediation process faces significant challenges due to difficulty in achieving uniform mixing of passivator particles and soil, and the primary issue is that the passivator particles and soil cannot be fully blended due to the limitations of mixing equipment, resulting in the passivator agglomeration, reduced soil utilization rates, and increased remediation costs. Meanwhile, human health will be increasingly endangered by the excessive use of passivators. Hence, to ensure effective remediation and protection of contaminated soil, it is necessary to explore the interactions among soil, passivation chemicals, and equipment, to improve the efficiency of soil remediation equipment, and to increase the uniformity of mixing between passivator particles and soil.

In this study, soil improvement with passivators based on in situ remediation was simulated via the Discrete Element Method (DEM). Specifically, the passivator was mixed into the soil for remediation using a rotary tiller. The soil and passivator were crushed and mixed at various travel speeds and blade roller speeds, with the goal of solve the mixing uniformity problem of soil and passivator, thereby contributing to the remediation of heavy metal-contaminated soil and providing optimized operating parameters for rotary tillers in agriculture applications.

2. STATE OF THE ART

Currently, contaminated soil is primarily remediated through physical, chemical, and biological methods. Passivators are mainly applied to chemical remediation, including biochar and lime. Numerous studies have demonstrated that these passivators can effectively eliminate or reduce heavy metals, such as cadmium and arsenic, in soil while improving soil nutrients, enzyme activity, and microbial populations, with the characteristics of low input costs, high remediation efficiency, fast remediation speed, and simple operation [11, 12]. Therefore, passivators have broad application prospects for soil pollution control.

For soil remediation involving mixing passivator particles with soil, numerous experiments must be conducted to accurately verify the interaction mechanisms among equipment, soil, and passivator particles. However, this process not only involves complex multifactor coupling effects but is also accompanied by high economic and time costs. As a result, numerical simulation based on the Discrete Element Method (DEM) has emerged as a valuable research tool, enabling scientists to explore these mechanisms more efficiently [13-15]. Referring to related research, Zhang et al. [16] used EDEM software to model rotary tiller–soil–straw interactions, analysing micromechanical behaviours and optimizing rotary blade design. Field experiments validated the model's accuracy, demonstrating its effectiveness for simulating soil and particle interactions. Arnaut et al. [17] designed a novel screw-mixing mechanical device based on the DEM to investigate particle mixing homogeneity. By simulating the movement and interactions of particles during the mixing process, the device analyses their distribution and mixing effects, providing strong references and support for the development of EDEM toward mixing uniformity. Li et al. [18] proposed a combined rotary and deep tillage method, which improved soil structure and crop yield but lacked systematic analysis of parameter optimization (e.g., travel speed and blade roller

speed). Sun et al. [19] used the Hertz–Mindlin contact model to simulate soil interactions with bionic and common deep ploughing, validating the model's reliability for multiparticle mixing analysis. Despite these advancements, there is limited data and theoretical analysis on how travel speed and blade roller speed affect the mixing uniformity of passivator particles and soil particles during in situ remediation. Further systematic research is needed to optimize soil remediation technology and enhance its effectiveness. This would provide a stronger theoretical foundation and technical support for improving remediation outcomes.

The mixing ability of rotary tillers depends on the soil–tool interaction. However, a plough pan may be formed during the operation of the rotary tiller, which can adversely affect soil moisture conservation and on the absorption and utilization of moisture in deep soil by plant roots [20]. In addition, the power demand and torque of different types of rotary tillers vary with their blade design, further influencing the travel speed of rotary tillers and the blade roller speed [21]. Therefore, an important link in soil remediation is to optimize the rotary blade to improve the working efficiency of rotary tillers.

The above research results mainly focused on passivators, EDEM software simulation, and rotary tiller operation. The passivators have been applied in various scenarios, but their uniformity when mixed with soil influences the exertion of their own characteristics. With contaminated soil as the research object, this study aims to improve in situ soil remediation efficiency. The overall structure of a rotary tiller was modelled using SolidWorks software, and the rotary tillage process of mixing and blending viscous soil and soil heavy metal passivator was simulated via EDEM software. This study provides a basis for optimizing the rotary tillage process and offers key theoretical guidance for solving the mixing uniformity problem of soil and passivator after rotary tillage.

The remainder of this study is organized as follows: Section 3 introduces the overall mechanical structure of the rotary tiller; Section 4 examines the effects of travel speed and blade roller speed on the mixing uniformity after primary and secondary rotary tillage; Section 5 reviews the features of the entire equipment, and summarizes the study. This study provides a valuable reference for the mixing uniformity of soil and passivator particles.

3. MATERIALS AND METHODS

3.1 Overall mechanical structure

As shown in Fig. 1, the horizontal rotary tiller mainly includes the power transmission part (universal joint, and gearbox), the working part (blade roller, and rotary blade), the frame part (main beam, side, and suspension device), and the soil covering and crushing device (supporting plate, and press wheel).
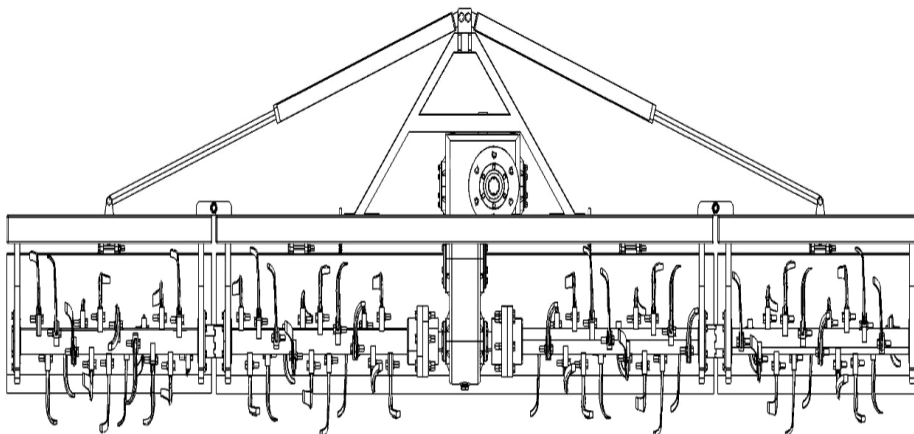

Figure 1: Schematic of the rotary tiller.

The main parts of the rotary tiller are made of IT245 65Mn. The blade and blade roller adheres to Rotary Tiller–Rotary Blades and Blade Holders (Chinese GB/T 5669-2017) [22], as shown in Fig. 2. Among them, the rotary blade measures 214 mm in length features an angle of 30°. The blade roller has a diameter of 90 mm in diameter, the spacing between blade holders is 110 mm, and the included angle between adjacent cutting edges within a single period of revolution is 22.5°. The blade roller is one of the core parts of the rotary tiller, and the rotary blade is installed on the blade roller.
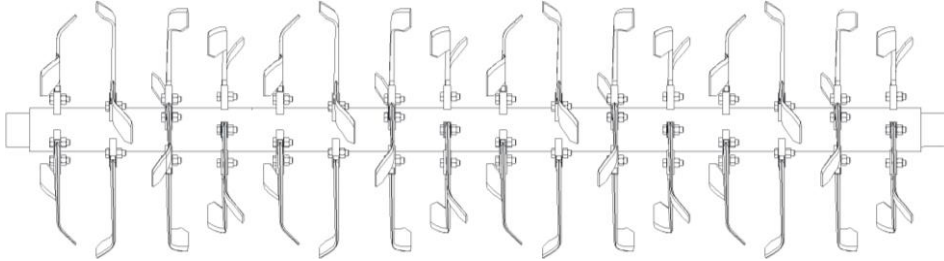
Figure 2: Schematic of the rotary blade roller.

3.2 Determination of the mixing uniformity

The coefficient of dispersion (C_v) is calculated through the following formula:

$$C_v = \frac{S}{\bar{X}} \times 100\% \qquad (1)$$

where S is the standard deviation of heavy metal passivator content in the soil sample; $\bar{X}$ is the mean value of heavy metal passivator content in the soil sample.

The uniformity of the mixture (M) is solved through C_v, as seen in Eq. (2):

$$M = 1 - C_v \qquad (2)$$

Mixing uniformity is one of the indexes indicating the operating quality of rotary tillers, while the mixing uniformity of discrete particles is generally reflected by the coefficient of dispersion [23]. The greater the coefficient of dispersion, i.e., standard deviation, the poorer the mixing uniformity of particles [24].

3.3 Simulation

In this study, a smooth solid sphere model was used to simulate the actual soil and the particle shape of a heavy metal passivator [25]. The single sphere particle model was selected from the EDEM software particle model library, and the soil particle radius was set to 5 mm, as shown in Fig. 3. The radius of heavy metal passivator particle was set to be randomly distributed within 1–5.6 mm, and the simulation model and random distribution parameters are illustrated in Fig. 4. The simulated particle material properties and the contact attribute parameters are listed in Table I and Table II [23].
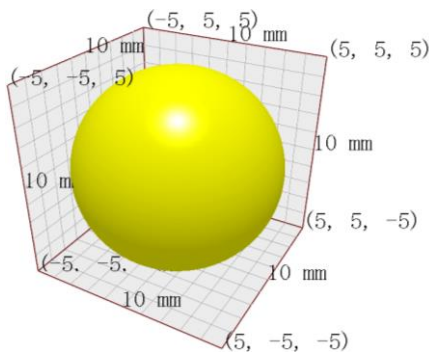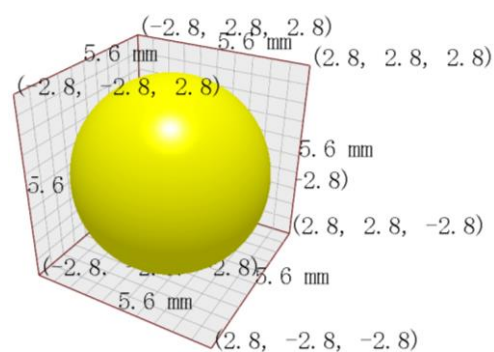

Figure 3: Soil particle model diagram.

Figure 4: Passivator model diagram.

Table I: Particle material property parameters [23].

Material	Poisson's ratio	Density (kg·m^{-3})	Shear modulus (Pa)
Soil	0.30	1385	2.79×10^8
Heavy metal passivator	0.25	1450	7.90×10^{10}
Steel	0.30	7850	7.90×10^{10}

Table II: Contact attribute parameters of interactive materials [23].

Interactive materials	Coefficient of restitution	Static friction coefficient	Rolling friction coefficient
Soil and soil	0.25	0.70	0.03
Soil and heavy metal passivator	0.25	0.60	0.02
Heavy metal passivator and heavy metal passivator	0.20	0.50	0.01
Soil and steel	0.50	0.50	0.01
Heavy metal passivator and steel	0.50	0.50	0.01

This study aims to investigate the mixing uniformity of passivator and soil using the rotary tiller. Given that soil contains water and is prone to cementation and agglomeration, this simulation was performed in contact models, such as linear translation kinematic, linear rotation kinematic, sinusoidal translation kinematic, and sinusoidal rotation kinematic. Viscous soil was simulated using the Hertz–Mindlin with JKR contact model, and the bonding energy was set to 8 J [26-29]. In accordance with the tillage width of the blade roller, the tillage depth was set to 250 mm. A soil trough with dimensions of $2000 \times 550 \times 300$ mm was established, and a virtual plane with dimensions of 2000×220 mm virtual plane was set up at the top of the soil trough as a particle factory for particle generation. The geometric simulation model is displayed in Fig. 5. According to reference [30], the maximum passivator addition amount of 20 kg was selected for the relevant research. In the experiment, the static generation method was adopted. The total number of particles was 357,000, comprising 320,000 soil particles (yellow particles) and 37,000 heavy metal passivator particles (laid on the soil surface). The created initial model is shown in Fig. 6.
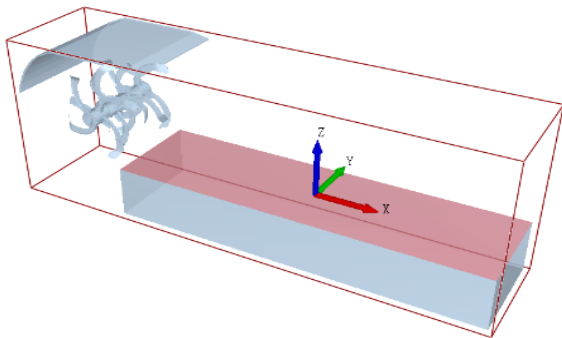

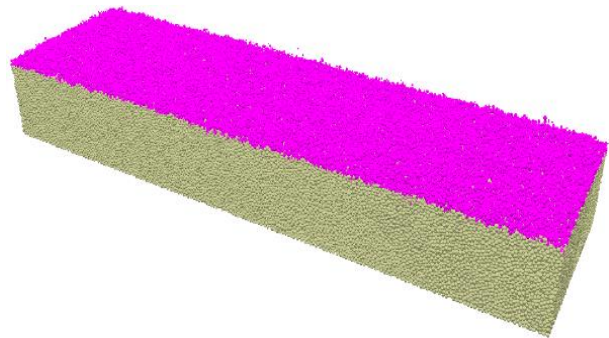Figure 5: Geometric simulation model.

Figure 6: Soil and heavy metal passivator model.

3.4 Experimental method

According to the Rotary Tiller (Chinese GB/5668-2017) [31], the travel speed for dry tillage was determined to be 2–3 km/h, the blade roller speed was 150–350 r/min, and the tillage depth was 250 mm. Two parameters, travel speed and blade roller speed, were selected as experimental factors, each with three levels. Therefore, a uniform design scheme was obtained, as shown in Table III. The simulation experiments were conducted sequentially using EDEM software, and the secondary rotary tillage was performed for a group of

parameters with the optimal rotary tillage results to explore whether the number of rotary tillage operations would affect the mixing uniformity of heavy metal passivator and soil.

Table III: Uniform design scheme for rotary tillage parameters of the rotary tiller.

No.	Travel speed (km/h)	Blade roller speed (r/min)
1	2.0	150
2	2.5	150
3	3.0	150
4	2.0	200
5	2.5	200
6	3.0	200
7	2.0	250
8	2.5	250
9	3.0	250

Given the instability of rotary tillage at the beginning of the simulation experiment, the simulation area of $500 \times 500 \times 250$ mm in the middle of the soil trough was designated for data extraction and recording. This area was divided into a $5 \times 4 \times 3$ grid, and the size of each grid was $100 \times 125 \times 100$ mm (only half of the top grids participated in data extraction; thus, the average particle number of one vertical grid and three grids was divided by 2.5) to facilitate data analysis and calculation. By reading the number of heavy metals passivator particles in each grid, the data of one longitudinal grid (three grids) were taken as one piece of sample data, the whole area was divided into 20 sample data points, and the coefficient of dispersion of heavy metal passivator particles on the 20 sample data points was calculated to reflect the mixing uniformity of heavy metal passivator particles in soil within this area. The grid partition is illustrated in Figs. 7 and 8.
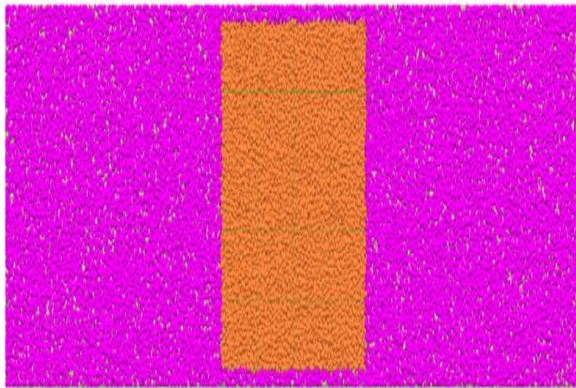

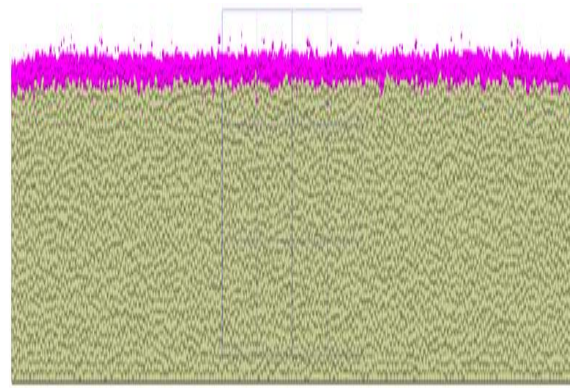Figure 7: Mesh delineation in the horizontal and vertical directions.

Figure 8: Delineation of the vertical grid.

4. RESULTS AND DISCUSSION

4.1 Mixing uniformity analysis

Mixing results in primary rotary tillage and analysis: Fig. 9 presents the sample uniformity data of nine groups of simulation experiments. Upon the comprehensive analysis of the data of mixing uniformity in each longitudinal depth, the mixing uniformity (the average value of 20 sample data points) in the whole grid area was accurately determined. When the blade roller speed was set at 150 r/min and the travel speed at 2, 2.5, and 3 km/h, the corresponding average mixing uniformities were 0.21, 0.17, and 0.09, respectively; when

set to 200 r/min, the values increased to 0.27, 0.14, and 0.12; when set to 250 r/min, the values increased to 0.32, 0.19, and 0.11.
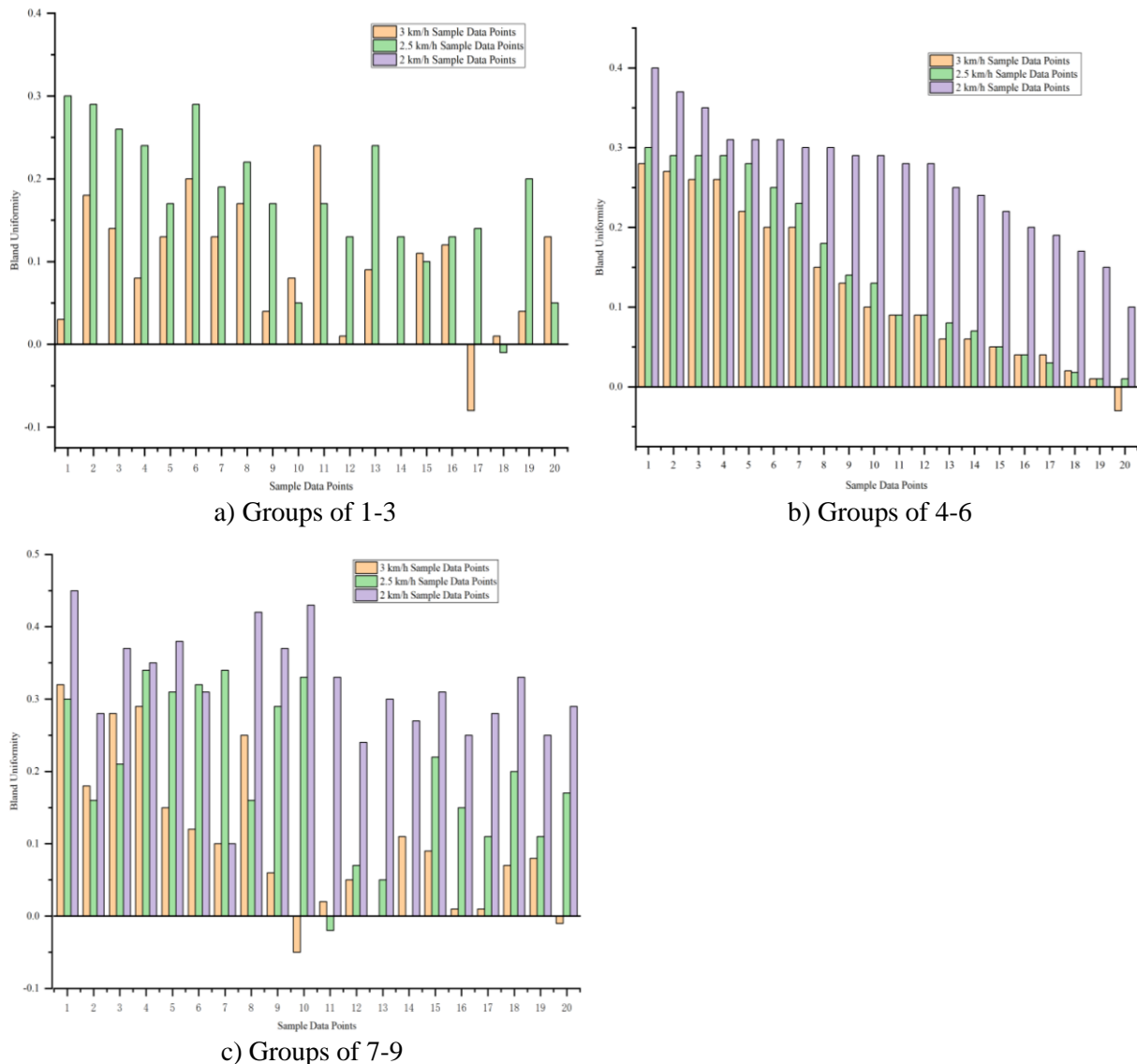

a) Groups of 1-3

b) Groups of 4-6

c) Groups of 7-9

Figure 9: Mixing homogeneity of simulated experimental samples.

Blade roller speed and mixing uniformity: The data indicate that the mixing uniformity did not always increase monotonically with the increase in the blade roller speed (from 150 r/min to 250 r/min) at the same travel speed. For example, when the travel speed was 3.0 km/h, the mixing uniformity increased from 0.09 (blade roller speed: 150 r/min) to 0.12 (blade roller speed: 200 r/min) and then decreased to 0.11 (blade roller speed: 250 r/min). At the travel speed of 2.5 km/h, the average mixing uniformity decreased from 0.17 (blade roller speed: 150 r/min) to 0.14 (blade roller speed: 200 r/min) and then increased to 0.19 (blade roller speed: 250 r/min). This result revealed that the increasing blade roller speed might increase the mixing uniformity, but an optimal speed existed, and when this speed was exceeded, the mixing uniformity might no longer increase or even decline.

Travel speed and mixing uniformity: Within the range of test conditions, the mixing uniformity could be improved by reducing the travel speed. Specifically, at the blade roller speed of 150 r/min, the travel speed decreased from 3.0 km/h to 2.0 km/h and the mixing uniformity grew from 0.09 to 0.21; at the blade roller speed of 200 r/min, the travel speed declined from 3.0 km/h to 2.0 km/h, and the mixing uniformity increased from 0.12 to 0.27;

when the blade roller speed was 250 r/min, the travel speed declined from 3.0 km/h to 2.0 km/h, and the mixing uniformity increased from 0.11 to 0.32. The possible reason is that a relatively low travel speed provides soil particles with more time for more thorough mixing and more even redistribution within the tillage area.

Interaction between blade roller speed and travel speed: At the same travel speed, the blade roller speed influenced the mixing uniformity to different degrees. In the experiments, the minimum mixing uniformity value observed was 0.09 (blade roller speed: 150 r/min, travel speed: 3 km/h) and 0.32 (blade roller speed: 250 r/min, travel speed: 2 km/h). At the travel speed of 2 km/h and the blade roller speed of 150 r/min, the average mixing uniformity was 0.21, which was lower than that at the same travel speed and the blade roller speed of 250 r/min, thus indicating the interaction between travel speed and blade roller speed, which jointly affected the mixing uniformity.

Influence mechanism of the blade roller speed: An elevation in the blade roller speed would increase the centrifugal force and tangential force of soil particles, thus improving the kinematic velocity and throwing distance of particles and promoting their mixing. However, an excessively high speed may lead to excessive crushing or compaction of soil particles and diminish the mixing uniformity on the contrary.

Influence mechanism of the travel speed: The decrease in the travel speed could lengthen the time for soil particles to act on the rotary tiller, facilitating the mixing and redistribution of particles and improving the mixing uniformity. Nevertheless, the operating efficiency might be reduced when the travel speed is too low.

Comprehensive influence of interactions: At a low travel speed, the mixing uniformity could be improved more remarkably by increasing the blade roller speed. The reason is that the low travel speed provides longer time for soil particles so that the increasing blade roller speed could fully exert its mixing action. On the contrary, the improvement effect of the blade roller speed on the mixing uniformity might be restricted at a relatively high travel speed, making it difficult to realize full mixing due to the short rotary tillage action borne by soil particles.

In summary, the mixing uniformity was more prominently influenced by the travel speed than by the blade roller speed. In the primary mixing process, the maximum mixing uniformity (0.32) was achieved at a travel speed of 2 km/h and a blade roller speed of 250 r/min. This result provided the optimal initial process condition for optimizing the secondary rotary mixing and establish a solid foundation for soil remediation and improvement.

Related data analysis of secondary rotary mixing: In the course of the initial rotary tillage and mixing operation, the optimal combination configuration was painstakingly identified by means of a comprehensive and systematic analysis and evaluation approach. Concurrently, the combination of the highest – achievable traveling operation velocity and the maximum cutter – roller rotational speed within the experimental framework was selected. Subsequently, a secondary rotary tillage and mixing operation was carried out for these two sets of parameters. The mixing uniformity values of twice mixing were compared, as shown in Fig. 10. The experimental data revealed that when the travel speed was 2 km/h and the blade roller speed was 250 r/min, the mixing uniformity increased from 0.32 to 0.82 after the secondary rotary tillage. When the travel speed was 3 km/h and the blade roller speed was 250 r/min, the mixing uniformity increased from 0.11 to 0.69 after the secondary rotary tillage. As shown in the figure, the mixing uniformity of heavy metal passivator after secondary rotary tillage was remarkably improved in comparison with that after primary rotary tillage.

Influence of travel speed on mixing uniformity: The data revealed that the decrease in travel speed (from 3 km/h to 2 km/h) was related to the improvement of mixing uniformity

under the fixed blade roller speed. This result can be attributed to the fact that the lower travel speed extended interaction time for soil particles to mix thoroughly and redistribute evenly, thus improving the mixing uniformity.

Variation trend of mixing uniformity: When the travel speed was 3 km/h, the average value of mixing uniformity indicates from 0.11 to 0.69 in primary rotary tillage, while when the travel speed was 2 km/h, the average mixing uniformity grew from 0.32 to 0.82 in primary rotary tillage. This variation trend indicated that the mixing uniformity was considerably influenced by the travel speed and secondary rotary tillage, with an optimal value of the travel speed that contributed to the maximum mixing uniformity.
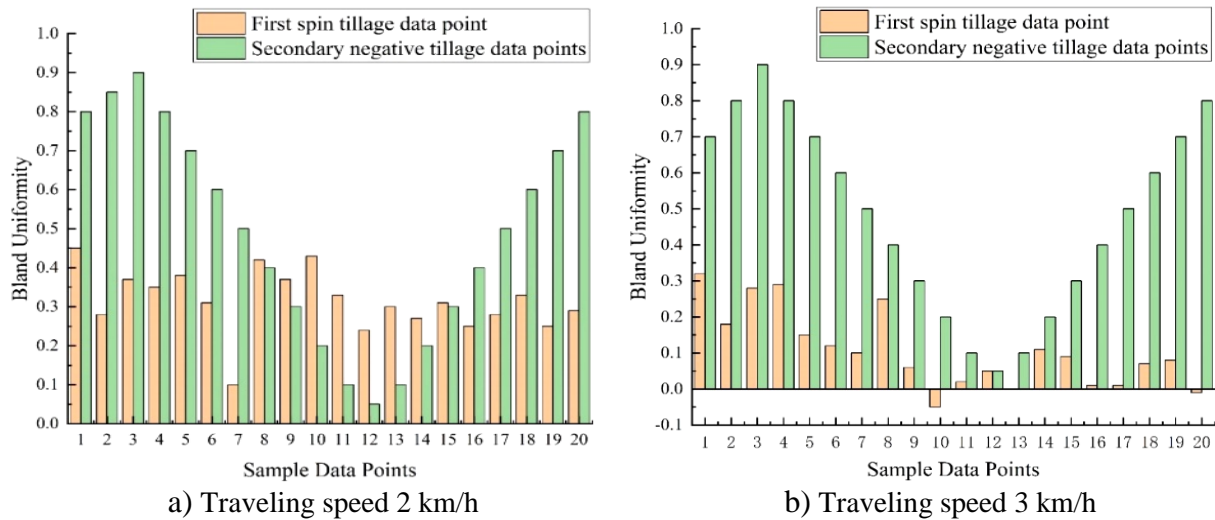

a) Traveling speed 2 km/h b) Traveling speed 3 km/h

Figure 10: Comparison of data from two rotary tillage samples blade roller speed 250 r/min.

Interaction between travel speed and blade roller speed: The mixing uniformity appears to be influenced by the interaction between the travel speed and blade roller speed. Despite the fixed blade roller speed, it could be inferred from the working principle of the rotary tiller that different blade roller speeds needed to be matched with different travel speeds to realize the optimal mixing uniformity.

Correlation between speed and uniformity: A low travel speed seems to correlate with the relatively high mixing uniformity. This correlation can be attributed to the fact that a low speed extended time available to soil particles for mixing, reducing the likelihood of soil stratification.

In summary, the travel speed after the secondary rotary tillage significantly impacts the mixing uniformity. Moreover, the secondary rotary tillage has remarkable advantages in improving the mixing uniformity, which can fully mix the passivator particles with soil.

4.2 Innovations and advantages

In this experiment, the mixing mode of secondary rotary tillage was proposed, aiming to enhance the integration of the passivator with the soil, with the following advantages:

Improvement of operating efficiency: Despite the increase in the number of operations, the operating time within unit area in secondary rotary tillage was effectively controlled through the reasonable operating parameter setting and mechanical configurations. Moreover, the increase in mixing uniformity facilitates smoother subsequent soil processing and planting operations because of the increase in mixing uniformity, thus improving the agricultural production efficiency on the whole.

Cost–benefit analysis: In the long run, the mixing uniformity of soil particles and passivator was improved after the secondary rotary tillage, which facilitated passivator

particles fully participating in the removal of heavy metals in soil, improved the overlimit status of heavy metals in soil, and provided an improved environment for crop growth. The yield growth compensates for the additional costs generated by the increasing number of operations. Additionally, the good soil structure and fertility level could reduce the use of fertilizers and pesticides, further decreasing the agricultural production cost and improving the economic benefit.

4.3 Application prospects and challenges

In the passivator–rotary tiller collaborative action system, the improvement of the soil structure by the rotary tiller created an extremely advantageous environment for the remediation of heavy metal-contaminated soil. The integration of the passivation process and the tillage operation not only optimizes the operational workflow but also substantially enhances the operational efficiency. Meanwhile, the passivation repair process was characterized by low equipment requirements, low energy consumption, and simple operation. On the premise of ensuring effective soil remediation, the economic cost of soil remediation could be considerably reduced by accurately regulating the amount of passivator applied.

In view of the uniqueness and complexity of plantation scenarios of different crops, the rotary tiller can be combined with other soil remediation equipment to achieve better remediation results. For example, in the vegetable plantation scenario, an integrated design of the steam sterilizer and rotary tiller can be considered. High-temperature steam is transported to the soil by a steam sterilizer, and harmful microorganisms and weed seeds in the soil can be effectively killed under the cooperation of the rotary mixing operation, thus achieving a good soil disinfection effect. In addition, combining the rotary tiller with the spray disinfection system is a feasible scheme. When the rotary tiller ploughs and stirs the soil, the spray disinfection system evenly sprays the disinfectant into the soil, which can effectively eliminate the pests and diseases in soil. These combined strategies not only represent the important future application direction in the field of soil remediation but also bring many challenges to the technical innovation and engineering practice in this field. This situation is worth exploring.

5. CONCLUSIONS

To improve the remediation effect of heavy metal pollution in soil, this study focuses on the rotary tillage technology in promoting the mixing uniformity of passivator particles and soil particles during efficient mixing and stirring. The rotary tiller was modelled using SolidWorks and subsequently simulated in EDEM software to thoroughly analyse the mixing process. Travel speed and blade roller speed were systematically studied to determine optimal operating conditions. And a simplified model was created for numerical simulation with a tillage depth of 25 cm. The optimal parameters identified were a travel speed of 2 km/h and a blade roller speed of 250 r/min. These settings achieved a mixing uniformity of 0.82 after secondary tillage, which represents 61 % improvement compared to that achieved after primary tillage. The study highlights that travel speed has a significant impact on mixing uniformity. However, it notes that the influence of the rotary tiller casing was not considered in this research, which could be a promising direction for future studies.

REFERENCES

[1] Gupta, P.; Biswas, S.; Tamrakar, G.; Sharma, S. (2024). Environmental health risk assessment of heavy metals contamination in the soils, *Transactions of the Indian Institute of Metals*, Vol. 77, 209-217, doi:10.1007/s12666-023-03092-z

[2] Joshi, N. C.; Gururani, P. (2024). A mini review on heavy metal contamination in vegetable crops, *International Journal of Environmental Analytical Chemistry*, Vol. 104, No. 20, 8708-8719, doi:10.1080/03067319.2023.2210058

[3] Kumar, V.; Sharma, A.; Kaur, P.; Singh Sidhu, G. P.; Bali, A. S.; Bhardwaj, R.; Thukral, A. K.; Cerda, A. (2019). Pollution assessment of heavy metals in soils of India and ecological risk assessment: a state-of-the-art, *Chemosphere*, Vol. 216, 449-462, doi:10.1016/j.chemosphere.2018.10.066

[4] Ministry of Environmental Protection of the People's Republic of China. (2014). National Soil Pollution Survey Bulletin, from *http://www.zhb.gov.cn/gkml/hbb/qt/201404/t20140417_270670.htm*, accessed on 15-08-2024

[5] Sheydaei, M. (2024). Investigation of heavy metals pollution and their removal methods: a review, *Geomicrobiology Journal*, Vol. 41, No. 3, 213-230, doi:10.1080/01490451.2024.2318227

[6] Ahmed, H. A. M.; Gouhar, A. S.; Janjua, M. N.; Alhafez, N. (2022). Estimation of some heavy metals contamination in waste newspapers, *Environmental Monitoring and Assessment*, Vol. 194, Paper 711, 13 pages, doi:10.1007/s10661-022-10215-4

[7] Deng, B.; Carter, R. A.; Cheng, Y.; Liu, Y.; Eddy, L.; Wyss, K. M.; Ucak-Astarlioglu, M. G.; Luong, D. X.; Gao, X.; JeBailey, K.; Kittrell, C.; Xu, S.; Jana, D.; Torres, M. A.; Braam, J.; Tour, J. M. (2023). High-temperature electrothermal remediation of multi-pollutants in soil, *Nature Communications*, Vol. 14, Paper 6371, 11 pages, doi:10.1038/s41467-023-41898-z

[8] Gavrilescu, M. (2022). Enhancing phytoremediation of soils polluted with heavy metals, *Current Opinion in Biotechnology*, Vol. 74, 21-31, doi:10.1016/j.copbio.2021.10.024

[9] Khalid, S.; Shahid, M.; Niazi, N. K.; Murtaza, B.; Bibi, I.; Dumat, C. (2017). A comparison of technologies for remediation of heavy metal contaminated soils, *Journal of Geochemical Exploration*, Vol. 182, Part B, 247-268, doi:10.1016/j.gexplo.2016.11.021

[10] Mathur, S.; Singh, D.; Ranjan, R. (2022). Remediation of heavy metal(loid) contaminated soil through green nanotechnology, *Frontiers in Sustainable Food Systems*, Vol. 6, Paper 932424, 13 pages, doi:10.3389/fsufs.2022.932424

[11] Nguyen, T.-B.; Sherpa, K.; Bui, X.-T.; Nguyen, V.-T.; Vo, T.-D.-H.; Ho, H.-T.-T.; Chen, C.-W.; Dong, C.-D. (2023). Biochar for soil remediation: a comprehensive review of current research on pollutant removal, *Environmental Pollution*, Vol. 337, Paper 122571, 11 pages, doi:10.1016/j.envpol.2023.122571

[12] Aziz, S.; Bibi, S.; Hasan, M. M.; Biswas, P.; Ali, M. I.; Bilal, M.; Chopra, H.; Mukerjee, N.; Maitra, S. (2024). A review on influence of biochar amendment on soil processes and environmental remediation, *Biotechnology and Genetic Engineering Reviews*, Vol. 40, No. 4, 3270-3304, doi:10.1080/02648725.2022.2122288

[13] Ahmadi, H. (2022). Analyzing the effectiveness of anti-slide piles for slope stabilization against seismic loading using discrete element method, *European Journal of Environmental and Civil Engineering*, Vol. 26, No. 16, 8133-8151, doi:10.1080/19648189.2021.2019617

[14] San, Y. L.; Li, Y. M.; Xiao, S. H.; Zhang, C. Y.; Liu, Y. B. (2024). Parameter optimization and analysis of plastic separator based on EDEM-Fluent, *International Journal of Simulation Modelling*, Vol. 23, No. 4, 622-633, doi:10.2507/IJSIMM23-4-701

[15] Shaikh, S. A.; Li, Y.; Ma, Z.; Chandio, F. A.; Tunio, M. H.; Liang, Z.; Solangi, K. A. (2021). Discrete element method (DEM) simulation of single grouser shoe-soil interaction at varied moisture contents, *Computers and Electronics in Agriculture*, Vol. 191, Paper 106538, 8 pages, doi:10.1016/j.compag.2021.106538

[16] Zhang, J.; Xia, M.; Chen, W.; Yuan, D.; Wu, C.; Zhu, J. (2023). Simulation analysis and experiments for blade-soil-straw interaction under deep ploughing based on the discrete element method, *Agriculture*, Vol. 13, No. 1, Paper 136, 20 pages, doi:10.3390/agriculture13010136

[17] Arnaut, L. R.; Moglie, F.; Bastianelli, L.; Primiani, V. M. (2017). Helical stirring for enhanced low-frequency performance of reverberation chambers, *IEEE Transactions on Electromagnetic Compatibility*, Vol. 59, No. 4, 1016-1026, doi:10.1109/TEMC.2016.2641386

[18] Li, J.; Chen, L.; Zhang, C.; Ma, D.; Zhou, G.; Ning, Q.; Zhang, J. (2024). Combining rotary and deep tillage increases crop yields by improving the soil physical structure and accumulating organic carbon of subsoil, *Soil and Tillage Research*, Vol. 244, Paper 106252, 9 pages, doi:10.1016/j.still.2024.106252

[19] Sun, J.; Wang, Y.; Ma, Y.; Tong, J.; Zhang, Z. (2018). DEM simulation of bionic subsoilers (tillage depth >40 cm) with drag reduction and lower soil disturbance characteristics, *Advances in Engineering Software*, Vol. 119, 30-37, doi:10.1016/j.advengsoft.2018.02.001

[20] Szczepanek, M.; Piekarczyk, M.; Błaszczyk, K. (2024). Spatial distribution of soil macroelements, their uptake by plants, and green pea yield under strip-till technology, *Agronomy*, Vol. 14, No. 4, Paper 711, 22 pages, doi:10.3390/agronomy14040711

[21] Zhang, G.; Zhang, Z.; Xiao, M.; Bartos, P.; Bohata, A. (2019). Soil-cutting simulation and parameter optimization of rotary blade's three-axis resistances by response surface method, *Computers and Electronics in Agriculture*, Vol. 164, Paper 104902, 10 pages, doi:10.1016/j.compag.2019.104902

[22] China Machinery Industry Federation (2017). Rotary tiller tool and tool holder GB/T 5669-2017, from *http://c.gb688.cn/bzgk/gb/showGb?type=online&hcno=C4B7105A94E886B2D0DA8C509 510F3CF*, accessed on 15-08-2024

[23] Wang, Z.; Zhu, T.; Wang, Y.; Yang, S.; Ma, F.; Li, X. (2024). Simulation and analysis of soil homogenization drills based on discrete element method and response surface methodology, *Particuology*, Vol. 88, 128-148, doi:10.1016/j.partic.2023.09.004

[24] Deng, T.; Fisonga, M.; Ke, H.; Li, L.; Wang, J.; Deng, Y. (2024). Mixing uniformity effect on leaching behaviour of cement-based solidified contaminated clay, *Science of The Total Environment*, Vol. 908, Paper 167957, 11 pages, doi:10.1016/j.scitotenv.2023.167957

[25] Yazdani, E.; Hashemabadi, S. H.; Taghizadeh, A. (2021). Investigation of particulate bed dynamics inside a rotating drum using discrete element method, *Particulate Science and Technology*, Vol. 39, No. 8, 917-927, doi:10.1080/02726351.2020.1870595

[26] Marveggio, P.; Redaelli, I.; di Prisco, C. (2022). Phase transition in monodisperse granular materials: how to model it by using a strain hardening visco-elastic-plastic constitutive relationship, *International Journal for Numerical and Analytical Methods in Geomechanics*, Vol. 46, No. 13, 2415-2445, doi:10.1002/nag.3412

[27] Du, J.; Xia, J.; Wu, H.; Xu, W. (2020). An investigation of the performance of waterjet for lotus root digging device: simulation and experiment, *International Journal of Fluid Machinery and Systems*, Vol. 13, No. 1, 160-166, doi:10.5293/ijfms.2020.13.1.160

[28] Lu, J.-M.; Li, C.-F.; Cao, G.-C.; Hu, S.-M. (2022). Simulating fractures with bonded discrete element method, *IEEE Transactions on Visualization and Computer Graphics*, Vol. 28, No. 12, 4810-4824, doi:10.1109/TVCG.2021.3106738

[29] Mauser, N. J.; Zhang, Y.; Zhao, X. (2020). On the rotating nonlinear Klein–Gordon equation: nonrelativistic limit and numerical methods, *Multiscale Modeling & Simulation*, Vol. 18, No. 2, 999-1024, doi:10.1137/18M1233509

[30] Ye, S.; Wang, L.; Liu, T. (2022). Study of solidification and stabilization of heavy metals by passivators in heavy metal-contaminated soil, *Open Chemistry*, Vol. 20, No. 1, 1-9, doi:10.1515/chem-2021-0101

[31] China Machinery Industry Federation (2017). Rotary cultivator GB/T 5668-2017, from *http://c.gb688.cn/bzgk/gb/showGb?type=online&hcno=C4A5376BA5C4F93CF353E9BD73DB7 E99*, accessed on 15-08-2024